NASA

Technical Memorandum 82167

Calculation of Surface Temperature and Surface Fluxes in the GLAS GCM

Y. C. Sud and J. A. Abeles

July 1981

Laboratory for Atmospheric Sciences
Modeling and Simulation Facility

National Aeronautics and
Space Administration

Goddard Space Flight Center
Greenbelt, Maryland 20771

CALCULATION OF SURFACE TEMPERATURE AND SURFACE FLUXES IN THE GLAS GCM

Yogesh C. Sud

and

James A. Abeles

Sigma Data Services Corporation
(Contract No. NAS5-25900)
c/o NASA Goddard Space Flight Center
Greenbelt, MD 20771

and

Laboratory for Atmospheric Sciences
NASA Goddard Space Flight Center
Greenbelt, MD 20771

July 1981

ABSTRACT

The GLAS model's surface fluxes of sensible and latent heat were found to exhibit strong 2-δt oscillations at the individual grid points as well as in the zonal and hemispheric averages. In addition, it was pointed out by Charney *et al.* (1977) that a basic weakness of the GLAS model has been its lower evaporation over oceans and higher evaporation over land in a typical monthly simulation. On examining the planetary boundary layer (PBL) parameterization, it appeared that the calculation of surface temperature and the use of *ad hoc* constants in the eddy diffusivity calculation for the mixed layer were primarily responsible for these deficiencies.

The GLAS model PBL parameterization has been changed to calculate the mixed-layer temperature gradient by solution of a guadratic equation for a stable PBL and by a curve-fit relation for an unstable PBL. The basic formulae used to determine the drag coefficient, its stability dependence, and the effect of moisture on the temperature gradient remain unchanged. The new PBL parameterization yields surface temperature and surface fluxes without any 2-δt oscillation. Also, the geographical distributions of the surface fluxes are improved.

The parameterization presented here is incorporated into the new GLAS climate model. Some results which compare the evaporation over land and ocean between old and new calculations are appended.

INTRODUCTION

In a series of climate simulations with the GLAS GCM, it was found by Charney et al. (1977) that the zonally averaged monthly mean evaporation was less than observed over the oceans and greater than observed over the land. This weakness in the model has persisted consistently in all summer and winter simulations. We also noticed a 2-6t oscillation in the evaporation. This oscillation was evident in the zonal and hemisphere averages as well as at individual grid points. At this point, a systematic examination of the boundary layer parameterization was undertaken. Before discussing the details of this problem, we provide the following background on the GLAS PBL parameterization.

The present PBL parameterization was originally developed by Katayama† (1972). Later, the Katayama parameterization was modified by Somerville et al. (1974), who introduced the formulation (Deardorff, 1967) for the eddy diffusivity of the mixed layer. For some reason, not discussed by Somerville et al. (1974), the original constants used by Deardorff were somewhat modified. In this parameterization, the PBL is assumed to be made up of two layers: the surface layer and the mixed layer. The surface variables are defined at the interface between these layers. These are surface temperature T_s, the surface humidity q_s, and surface wind components U_s and V_s. The surface layer is very shallow; its depth is about 10-50 m. For this reason, its heat and moisture capacities are negligible. Therefore, T_s is an equilibrium temperature determined by the

† As described by Arakawa (1972) in the Design of UCLA General Circulation Model.

requirement that the fluxes of the surface layer and the mixed layer are consistent with each other. Similarly, surface humidity is determined by requiring equality of the surface layer moisture flux and the mixed-layer moisture flux.

Since surface temperature is not known a priori, in the old parameterization, the surface temperature from the previous time step was used to calculate the new fluxes, which were then used to obtain the new surface temperature. The final surface temperature was then the average of the old and the new values. Finally, this surface temperature was used to recalculate the surface fluxes. In affect, it amounts to one cycle of iteration. Even with all this averaging, a 2-δt oscillation in the surface temperature occurred. This gave rise to corresponding oscillations in the surface fluxes.

GOVERNING EQUATIONS

In the GLAS model, a stable PBL forms whenever the ground is cooler than the air, and an unstable PBL forms whenever the ground is warmer than the air. The air temperature used in this comparison is the potential temperature at the lowest model level, level 9 of the GCM, which is nominally 945 mb. Of course, for saturated air a correction is necessary to account for the lapse rate modification by moisture. The parameterization proposed here is based on a unique solution for the surface temperature, which corrects the 2-δt oscillation found in the old parameterization. An "analytic" solution for T_s is obtained

for the stable PBL, and a curve-fit solution for T_s is obtained for the unstable PBL. The basic quantities and useful variables are defined below:

T_g = ground temperature, K

q_g^* = saturation mixing ratio at the ground

T_9, θ_9 = physical and potential temperature of layer 9 in the model

q_g = mixing ratio at level 9 of the atmosphere

q_s = surface mixing ratio

U_s, V_s = surface U,V winds, in ms^{-1}

U_9, V_9 = level 9 U,V winds, in ms^{-1}

$W_s = U_s^2 + V_s^2$

K = Eddy transport coefficient of the mixed layer cal $m^{-1}k^{-1}$

L = latent heat of evaporation cal g^{-1}

C_p = specific heat at constant pressure

R = gas constant

$\kappa = R/C_p$

ε = ratio of molecular weights of water and air

The temperature difference across the mixed layer, $\delta\theta$, is modified to reflect the moist adiabatic lapse rate as follows:

The lapse rate for dry atmosphere is obtained from

$$-\frac{dT}{dz} = \Gamma_d = \frac{g}{c_p} \quad . \tag{1}$$

For the saturated air, the relation is

$$-\frac{dT}{dz} = \Gamma_s = \frac{g}{C_p}\left[\frac{1 + R\frac{L}{T_s}\frac{q^*}{}}{1 + \frac{L}{Cp}\frac{de}{dT}}\right] . \tag{2}$$

If the relative humidity in the real atmosphere is r_s, then Γ_{rs} is obtained by linear interpolation as follows:

$$\Gamma_{r_s} = (1 - r_s)\ \Gamma_d + r_s\ \Gamma_s \quad , \tag{3}$$

The above calculation assumes that the saturated air mass in the PBL regime of a grid cell is proportional to the relative humidity of air involved.

Or

$$\Gamma_{r_s} = \Gamma_d + r_s \frac{g}{C_p} \left[1 - \frac{\frac{L}{kCp} \frac{q_s^*}{Ts}}{1 + 5418 \frac{L}{C_p} \frac{q_s^*}{T_s}} \right] \tag{4}$$

Equation (4) follows from (3) and (2) with the use of the following additional relations:

$$q_s^* = \varepsilon.(10^{9.4051-2353/T})/p$$

and $e_s = q_s^* p/\varepsilon$

Multiplying (4) by the boundary layer height, and using

$$\Delta T_c = \Gamma_{r_s} \Delta Z_B \tag{5a}$$

$$\Delta T_d = \Gamma_d\ \Delta Z_B \quad , \tag{5b}$$

and

$$\gamma_c = r_s \frac{g}{C_p}\ \Delta Z_B\ [1 - \{1 + \frac{L}{Cpk}\ (q_s^*/Ts)\}/\{1 + 5418\ Lq_s^*/C_pT_s\}] \tag{5c}$$

we obtain

$$\Delta T_c = \Delta T_d + \gamma_c \quad . \tag{6}$$

To solve the PBL equations to obtain the surface temperature, we define

$$\Delta\theta = T_g - \theta_9 \quad , \tag{7a}$$

$$\delta\theta = T_s - \theta_9 \quad , \tag{7b}$$

and $$\Delta\theta - \delta\theta = T_g - T_s \quad , \tag{7c}$$

where $\theta_9 = T_9 \, (p_s/p_9)^{\kappa}$ and $\theta_g \equiv T_g$ and $\theta_s \equiv T_s$ (see Fig. 1).

We solve for $\delta\theta$ for a given $\Delta\theta$, then obtain T_s from (7c).

The drag coefficient, C_D (also equal to heat transport coefficient), is a linear function of surface geopotential over land and a linear function of surface wind over the oceans. Assuming that C_D is known for a given grid cell, the surface heat flux, F_s, may be obtained as follows:

$$F_s = \rho . C_p \, D_R \, (\theta_g - \theta_s) \tag{8}$$

where

$$D_R = C_D W_s^{\,3} / \{W_s^{\,2} - 7x(\Delta\theta - \delta\theta)\} \qquad \text{if } T_g < T_s \quad , \tag{9a}$$

or

$$D_R = C_D \{W_s + \sqrt{(\Delta\theta - \delta\theta)}\} \qquad \text{if } T_g > T_s . \tag{9b}$$

The mixed-layer heat flux, F_{ml}, is given by

$$F_{ml} = - \rho C_p \, K/Z_B(\Delta T - \Delta T_c) \ , \qquad (10)$$

where K is the eddy diffusivity of the mixed layer. There are separate parameterizations for the calculation of K for the stable and unstable PBL's as follows:

For the stable case

$$K = 60./(1 + 40.*R_i) \ , \qquad (11)$$

where Bulk Richardson number, R_i, is defined as

$$R_i = - \delta\theta g z_b/[\theta_g * \{(U_9-U_s)^2 + (V_9 - V_s)^2\}] . \qquad (12)$$

For the unstable case

$$K = 60. + 100. \ [1 - \exp(-1.2 \ \frac{\partial \theta}{\partial z})] \ . \qquad (13)$$

By equating F_s and F_m , we find that

$$D_R(\theta_g - \theta_s) = -K/Z_B \ (\Delta T - \Delta T_d - \gamma_c) = K/Z_B(\delta\theta + \gamma_c). \qquad (14)$$

Here we have used $\Delta T - \gamma T_d - \gamma_c = (T_9 - T_s) - (T_9 - T_s)_{da} - \gamma_c$

$$= -[(T_s - T_{s_{da}}) + \gamma_c]$$

$$= -(\delta\theta + \gamma_c) \ .$$

From (14), and with given values of θ_g, T_9, θ_9, γ_c, D_R, and K, it is now possible to determine $\delta\theta$ and θ_s. The case for an unstable PBL is solved by a curve-fit relation between

$\delta\theta = f(\Delta\theta, C_D, W_s)$. The case for a stable PBL is determined exactly by solving a quadratic equation in $\delta\theta$.

(a) Solution for $\delta\theta$ (Stable Case)

A stable case is obtained by using Equations (14), (9a), and (11).

$$\delta\theta = \frac{\{C_D W_s^3/[W_s^2 - 7\,(\Delta\theta - \delta\theta)]\}\Delta\theta}{C_D W_s^3/[W_s^2 - 7(\Delta\theta - \delta\theta)] + \frac{1}{Z_B} \cdot [60/(1 - 40 \cdot \delta\theta g Z_B/\theta_g D_w^2)]},$$

where $D_w^2 = (U_9 - U_s)^2 + (V_9 - V_s)^2$

which rearranges to

$$\underbrace{(7 \times 60/Z_B c_D W_s^3 - 40 g Z_B/\theta_g D_w^2)}_{A}\delta\theta^2 + \underbrace{(1 + 60/Z_B c_D W_s - 7\times 60./Z_B c_D W_s^3 + 40 g z_B c_D/\theta g D_w^2)}_{B}\delta\theta = \Delta\theta \qquad (15)$$

from which $\delta\theta$ may be obtained. If A approaches zero in the quadratic equation $A\delta\theta^2 + B\delta\theta = \Delta\theta$, the limiting solution is

$$\delta\theta = -\Delta\theta/B(1 - A.\Delta\theta/B^2). \qquad (16)$$

In the above formulation, the boundary layer height Z_B is of the order of 500 m. However, a stable PBL is generally shallow. Its height is of the order of 100 m. In order to reflect the difference in height, the constant '40' is changed to '8.'

A limiting value of K = 2.0 is reached when the limiting critical Richardson Number 3.05 is attained (Deardorff, 1967). Accordingly, the minimum value of $\delta\theta$ is obtained by combining (14), (9a) and (11) to give

$$\delta\theta = \Delta\theta/[1. + (K_{min}/Z_B C_D W_s)(1-7.\Delta\theta/W_s^2)] \ . \qquad (17)$$

(b) Solution for $\delta\theta$ (Unstable Case)

In an unstable case, (14), (9b) and (13) must be solved. Since (13) is transcendental, an exact solution is not possible. Hence, an attempt is made to obtain $\delta\theta$ as a function of $\Delta\theta$, W_s, and C_D, for a range of values. Figures (2a), (2b), and (2c) show $\delta\theta$ as a function of $\Delta\theta$ for values of C_D between .001 and .005 and surface wind magnitudes of 2-12 ms^{-1}. In all the graphs, the lines are the curve-fit solutions to match the points which are exact calculations. From these solutions, graphs are obtained for $\delta\theta/\Delta\theta$ versus C_D, for various values of the winds (Figure 2d) and $\delta\theta/\Delta\theta$ versus surface wind for various values of C_D (Figure 2e).

A simple functional form to obtain curve-fit relation $\delta\theta$ and $\Delta\theta$, C_D and W_s can be derived. Obviously,

$$\delta\theta = f(\Delta\theta, C_D, W_s). \qquad (18)$$

However, since $\delta\theta$ is linear with $\Delta\theta$, a suitable functional form will be

$$\delta\theta/\Delta\theta = f(C_D, W_s). \qquad (19)$$

But at $W_s = 0$, $\delta\theta/\Delta\theta \neq 0$. Therefore, assume the functional form to be

$$\delta\theta/\Delta\theta = f_1(C_D, W_s) + f_2(C_D). \qquad (20)$$

Some preliminary calculations indicate a general form to be

$$\delta\theta/\Delta\theta = af_1(C_D^n, W_s) + f_2(C_D), \tag{21}$$

which was approximated by

$$\delta\theta/\Delta\theta = A_1 W_s C_D^{1/2} + A_2 C_D, \tag{22}$$

where A_1 and A_2 are arbitrary constants. Using the method of least-squares, the constants A_1 and A_2 were found to be 0.1382 and 13.67, respectively. Therefore, the final form of the relation between $\delta\theta$ and $\Delta\theta$ is:

$$\delta\theta = (0.1382 \times W_s \times C_D^{1/2} + 13.67\ C_D)\Delta\theta. \tag{23}$$

(c) Wind Field Modification by Surface Drag

The surface drag force acting on a grid cell produces a change in the momentum of the air at level 9, which, in the GLAS parameterization, is the only layer directly affected. Also, for Arakawa Grid B (Arakawa, 1972), the wind fields are defined at the secondary points, whereas the drag force is calculated at the primary points. In the old code, first the wind fields were interpolated to primary points, then momentum deficit was calculated for the interpolated wind fields. This momentum deficit was then reinterpolated to secondary points. This back-and-forth interpolation does not allow a direct coupling between wind velocity and momentum deficit.

The effect of this interpolation may be minimal if every field is smoothly distributed. However, these wind fields are not smooth. Instead, large gradients are found,

particularly in the event of a growing 2-δx oscillation. The scheme of interpolation described above may result in spurious and sometimes systematic momentum transfers between grid cells, thus feeding these oscillations. Besides, and most importantly, any 2-δx pattern, if present, will be unaffected by friction. The new boundary layer calculation partly, if not completely, eliminates such a 2-δx oscillation. In the new procedure, first a factor, D_R, is calculated at each primary point, as before. It is then interpolated linearly to secondary points. The momentum deficit is now calculated by multiplying this factor by winds at level 9. Mathematically, the old method of obtaining $\Delta V_{i,j}$ was:

$$\Delta V_{Si,j} = 0.25 \{\Delta V_{Pi,j} + \Delta V_{Pi+1,j} + \Delta V_{Pi,j-1} + \Delta V_{Pi+1,j-1}\} \quad (24)$$

where $$\Delta V_{P,i,j} = - \frac{g}{\Delta P_{qi,j}} \cdot D_{Pi,j} \cdot \rho_{Pi,j} \cdot V_{Pi,j} \Delta t \quad (25)$$

It is replaced by the calculation given below:

First define $D'_{R_{Pi,j}}$ as follows

$$D'_{R_{Pi,j}} = - \frac{g}{\Delta P_{gi,j}} \cdot D_{R_{Pi,j}} \cdot \rho_{P_{i,j}} \cdot \Delta t \quad (26)$$

Now

$$D_{R_{si,j}} = 0.25 * \{D'_{R_{Pi,j}} + D'_{R_{Pi+1,j}} + D'_{R_{Pi,j-1}} + D'_{R_{Pi+1,j-1}}\} \quad (27)$$

and

$$\Delta V_{9Si,j} = D'_{R_{Si,j}} \cdot V_{9Si,j} \quad (28)$$

The symbols and indices used in the above equations are as follows: Indices i,j represent longitude and latitude. Suffix 'P' stands for variable defined at primary and 'S' for secondary points of the grid on Scheme B. P_9 is the mass of air in sigma level-9 in millibars. ρ is the density in 10^{-1} gm/cm^3. Δt is time step in seconds. The drag factor, D_R, is defined by (9a) and (9b) for a stable and an unstable PBL, respectively. Variable D'_{RS} is defined in Equation (28). Also, wind velocity updates are saved in an array. These are made simultaneously at the end.

ANALYSIS OF RESULTS

(1) First a time step invoking one call each of radiation and physics and three calls of hydrodynamics was completed to compare the results. The only striking difference was larger evaporative tendencies over oceans, and some large differences in surface temperature were noticed. Figure 3 shows the digitized maps of surface temperature differences. A large difference of 10-20°C may be seen in regions marked (I). These differences occur because in this region the air above the surface is very cold. The old model makes T_s close to the ground temperature, whereas the new model makes it close to the level-9 potential temperature. This is so because in the new calculation the eddy exchange coefficient has increased by an order of magnitude for the unstable atmosphere. The effect of this is to increase the forcing gradient of the surface fluxes. The larger temperature gradient, particularly over oceans,

increases D_R in equation (9b) and surface flux in equation (8). The same line of reasoning applies to moisture. However, over the land, increased surface fluxes will reduce the diurnal temperature oscillation. This suppresses evaporation in favor of increased sensible heat flux, because the diurnal oscillation of surface saturation humidity is several times the magnitude of the temperature oscillation. Thus, the net flux of moisture is reduced relative to the sensible heat flux.

(2) In a 1-day simulation, the 2-δt oscillation was eliminated. Figures (4a) and (4b) show the changes in the evaporation and sensible heat flux over land and ocean in the two hemispheres separately. The previous runs show a very noisy field compared to the new run. Consistent changes in daily averages of sensible heat flux and evaporation on individual grid points are now simulated.

SUMMARY

A new PBL parameterization has been tested with an exact solution for surface temperature instead of an iterative and time-averaged solution. Also incorporated is the original formulation of the eddy diffusion coefficient of Deardorff. The results from the new parameterization show desirable effects of increased evaporation over ocean and reduced evaporation over land. The proposed procedure of calculating surface temperature also eliminates the 2-δt oscillation in the surface fluxes of the old model. A short-range forecast revealed small but

beneficial effects on surface temperatures, sea level pressure, and geopotential heights at 500 mb.

ACKNOWLEDGMENTS

We would like to thank Dr. J. Shukla for encouraging us to independently solve this problem. Dr. D. Randall suggested the technique for wind field modification by surface drag. We sincerely thank him for his input. Also, we gratefully acknowledge support and interest expressed by Dr. M. Halem.

REFERENCES

Arakawa, A., 1972: Design of the UCLA atmospheric general circulation model. Tech. Report No. 7, Dept. of Meteor., Univ. of Calif. at Los Angeles.

Charney, J. G., W. J. Quirk, S. H. Chow, and J. Kornfield, 1977: A comparative study of the effects of albedo change on drought in semi-arid regions. J. Atmos. Sci., 34, 1366-1385.

Deardorff, J. W., 1967: Empirical dependence of the eddy coefficients for heat upon stability above the lowest 50 m. J. Appl. Meteor., 6, 631-643.

Halem, M., J. Shukla, Y. Mintz, M. L. C. Wu, R. Godbole, G. Herman, Y. Sud, 1979: Comparisons of observed seasonal climate features with a winter and summer numerical simulation produced with the GLAS general circulation model. Report of the JOC Study Conf. on Climate Models: Performance, Intercomparison and Sensitivity Studies, GARP Publ. Series No. 22, 207-253, WMO, Geneva, Switzerland.

Somerville, R. C. J., P. H. Stone, M. Halem, J. E. Hansen, J. S. Hogan, L. M. Druyan, G. Russell, A. A. Lacis, W. J. Quirk, and J. Tenenbaum, 1974: The GISS model of the global atmosphere. J. Atmos. Sci., 31, 84-117.

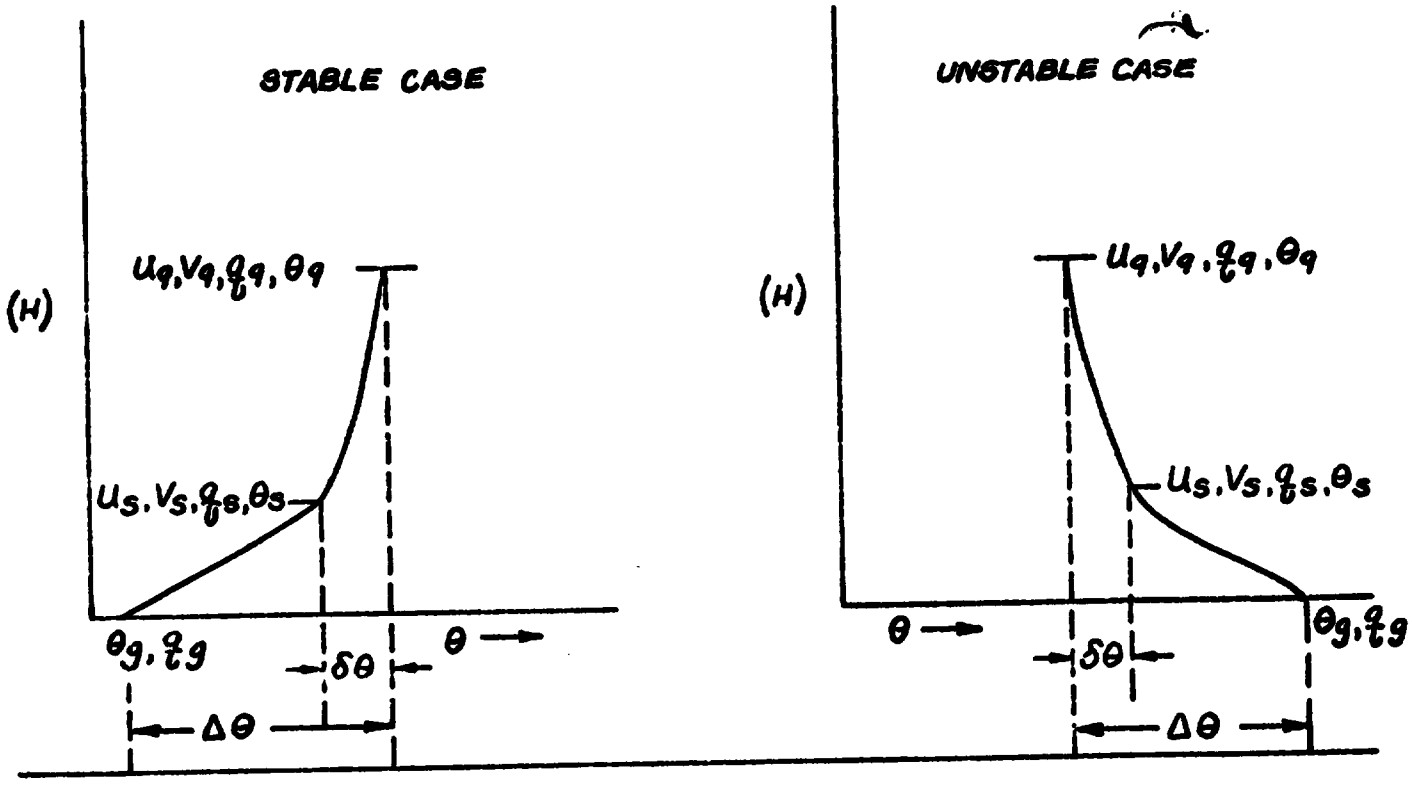

Figure 1. Schematic sketch of potential temperature profile in a boundary layer for stable and unstable PBL's.

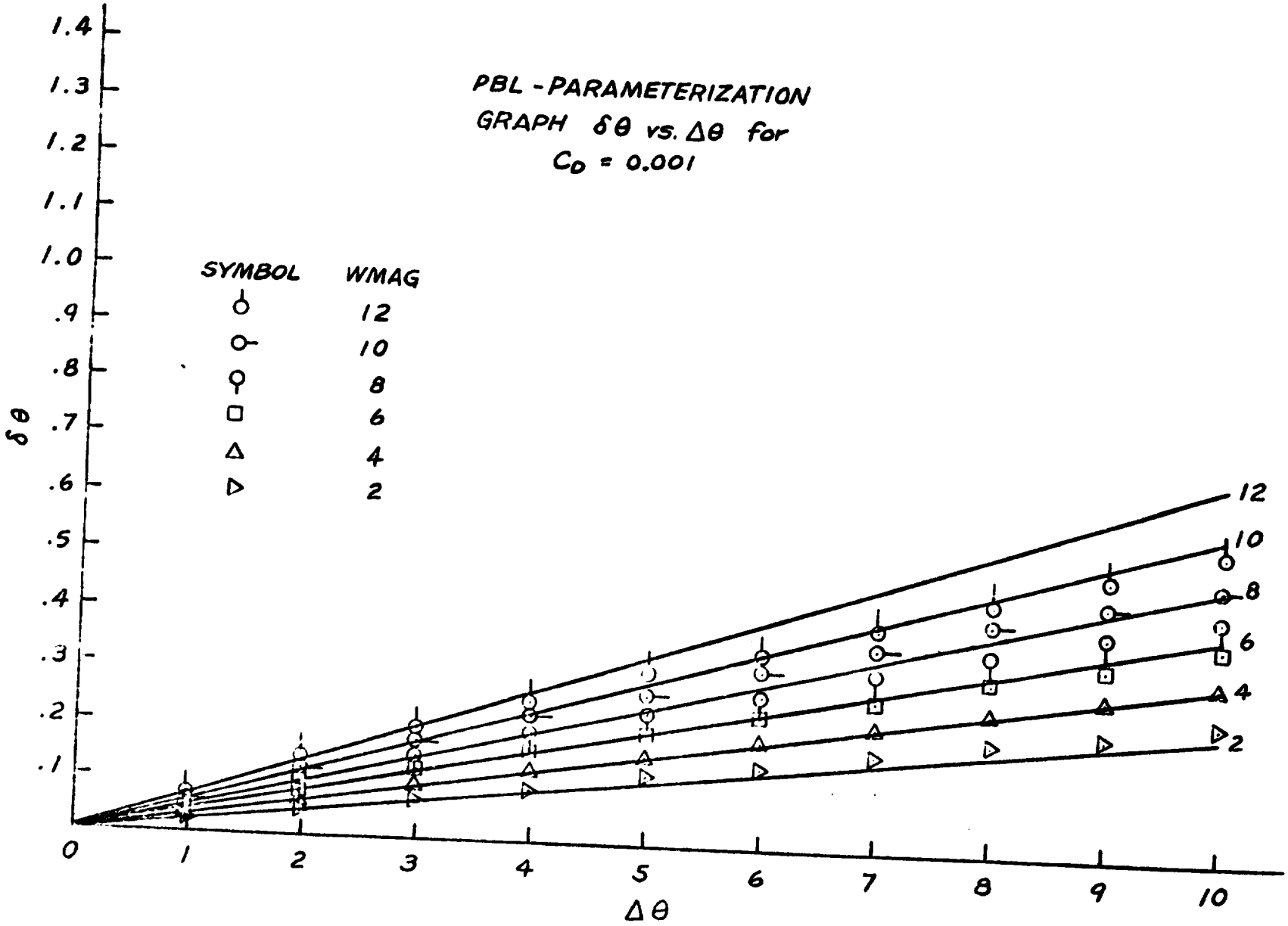

Figure 2(a). Graphs showing $\delta\theta$ vs. $\Delta\theta$ for various values of wind magnitudes and C_D=0.001 for unstable PBL. Exact calculations are points shown on curve fit solutions drawn as lines.

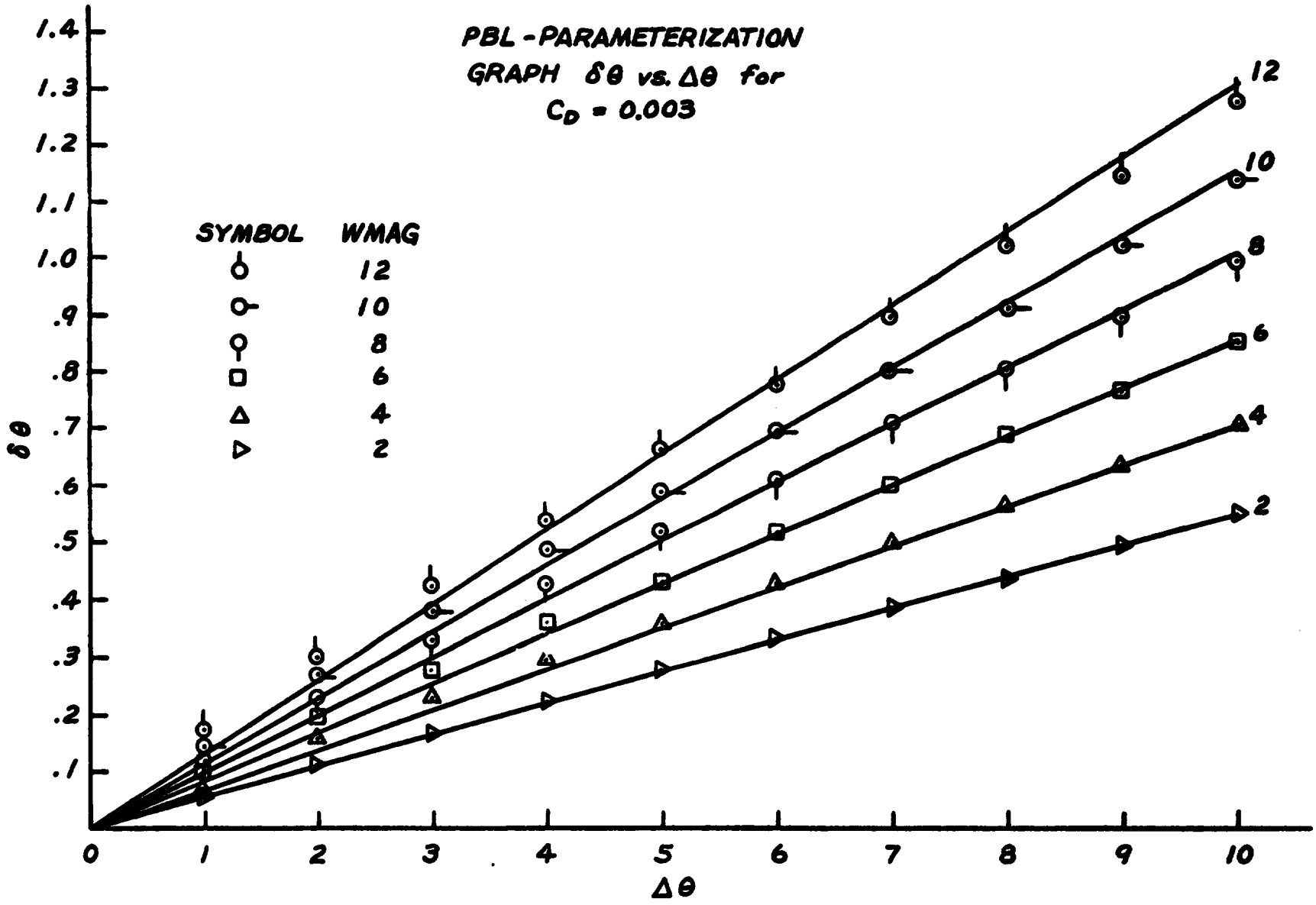

Figure 2(b). Same as Figure 2(a) except C_D=0.003 for unstable PBL.

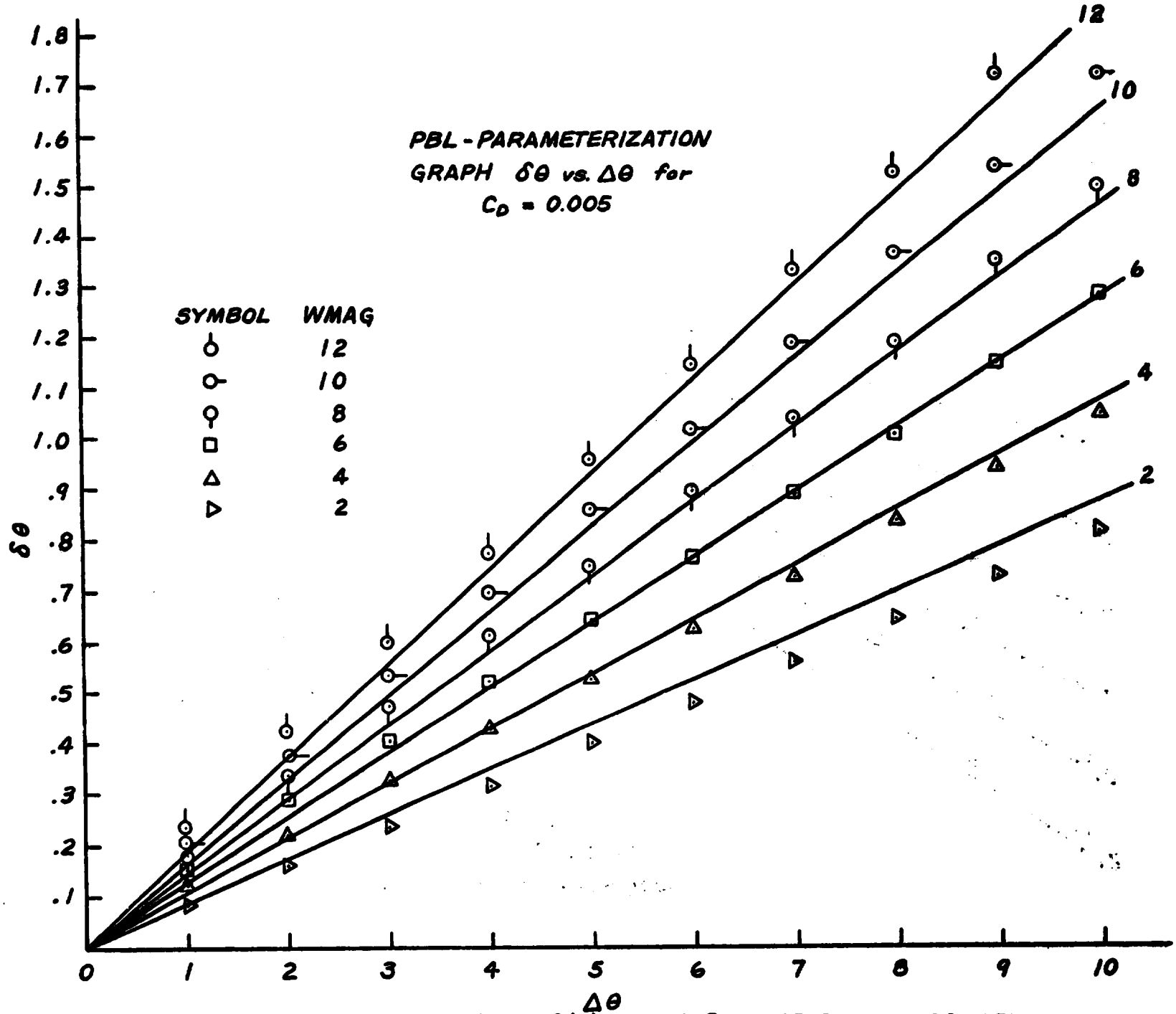

Figure 2(c). Same as Figure 2(a) except C_D=0.005 for unstable PBL.

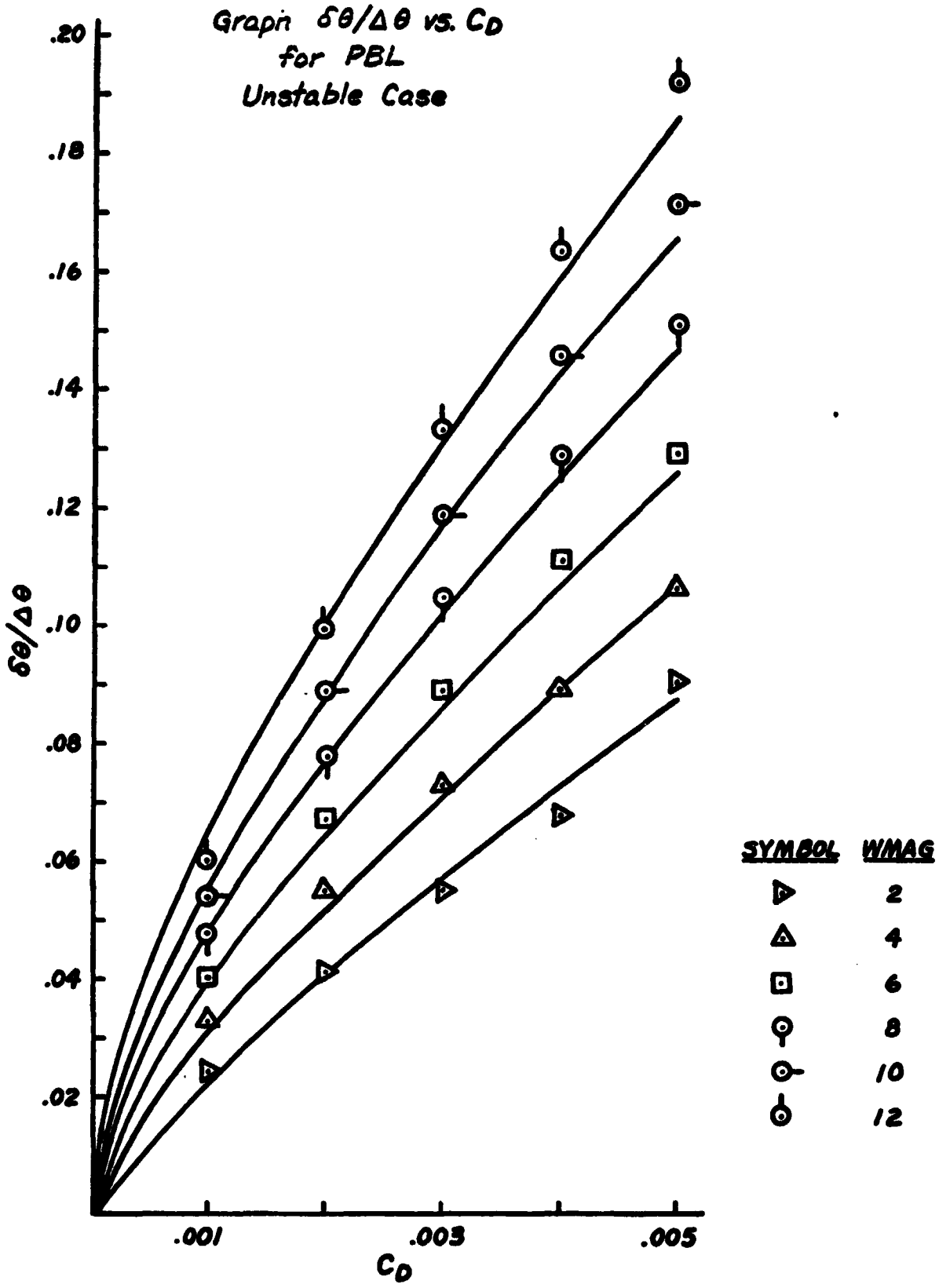

Figure 2(d). Graphs showing $\delta\theta/\Delta\theta$ vs. C_D for various wind magnitudes (for unstable PBL). Exact calculations are points shown on curve fit solutions drawn as lines.

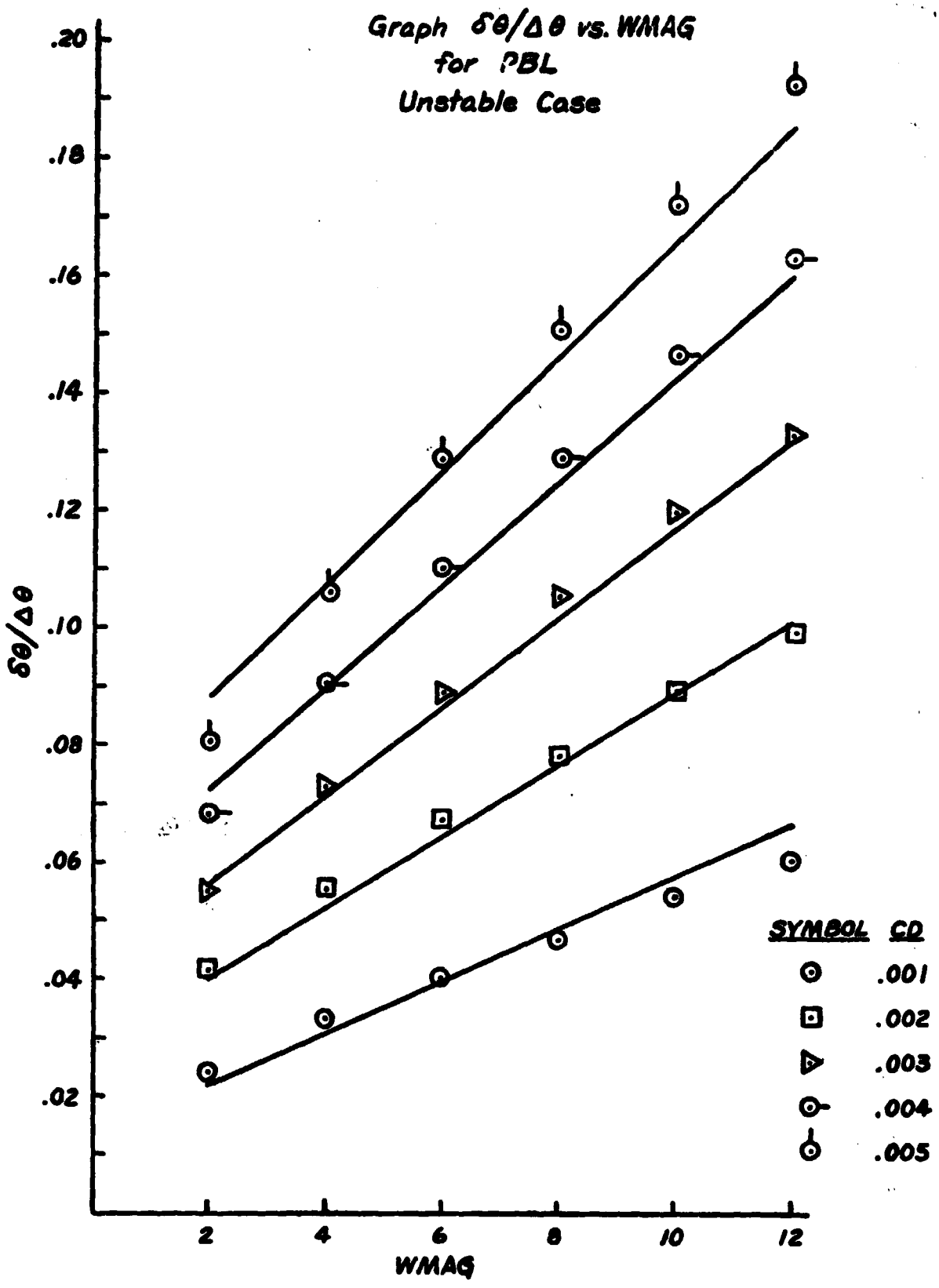

Figure 2(e). Graphs showing $\delta\theta/\Delta\theta$ vs. wind magnitude for various values of C_D (unstable PBL).

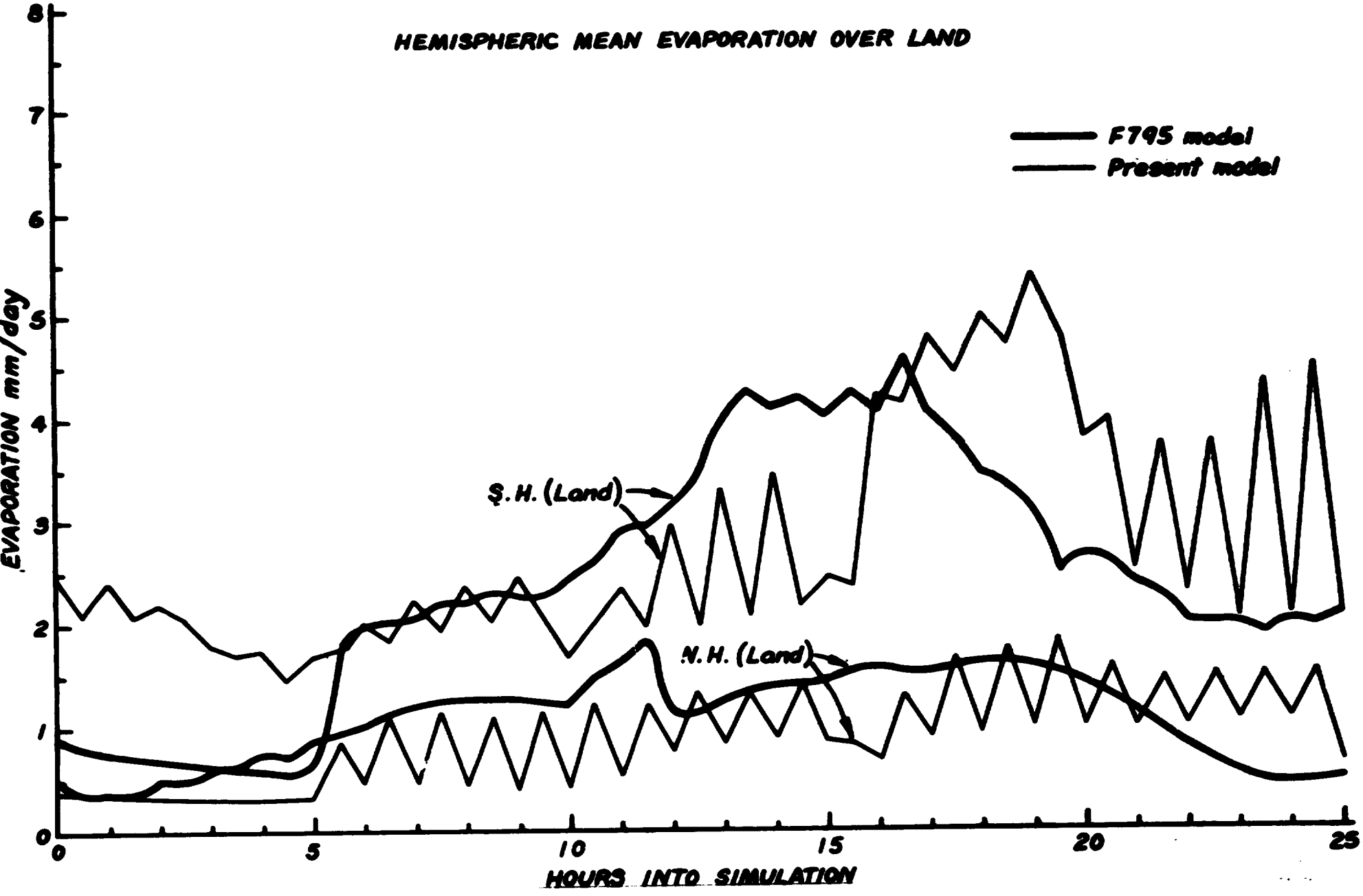

Figure 3(a). Hemispheric mean evaporation for the southern and northern hemispheres for 1-day simulation (land) old GLAS model vs. new calculation.

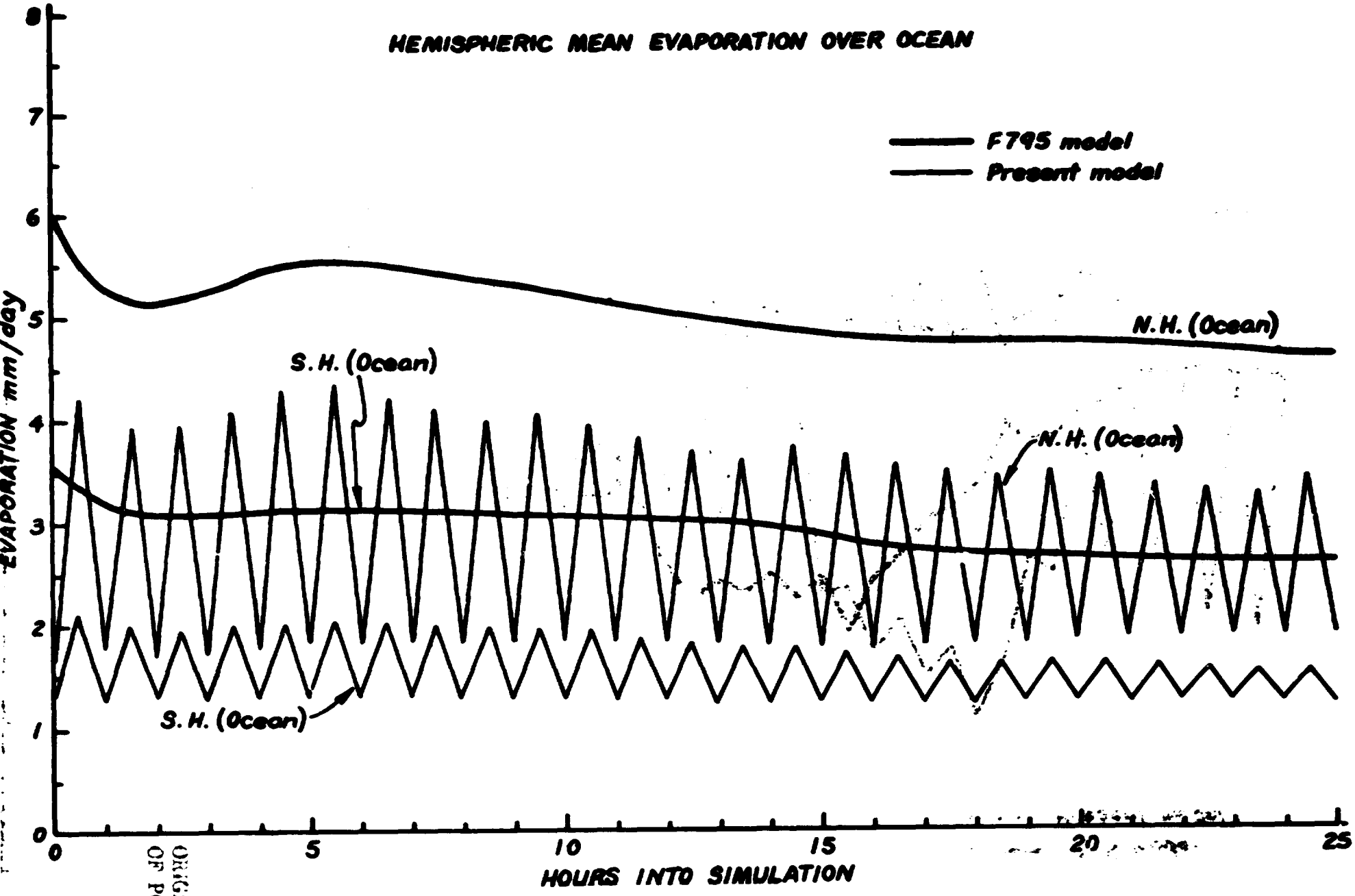

Figure 3(b). Same as Figure 3(a) except for 1-day simulation (ocean).